Published online November 27, 2005

Nucleic Acids Research, 2005, Vol. 33, No. 20 ***6515–6521***
doi:10.1093/nar/gki963

Synthesis of novel poly(dG)–poly(dG)–poly(dC) triplex structure by Klenow exo$^-$ fragment of DNA polymerase I

Alexander Kotlyar[1,2,*], Natalia Borovok[1], Tatiana Molotsky[1], Dmitry Klinov[3,4], Benjamin Dwir[3] and Eli Kapon[3]

[1]Department of Biochemistry, George S. Wise Faculty of Life Sciences, Tel Aviv University, Ramat Aviv, 69978 Israel, [2]Nanotechnology Center, Tel Aviv University, Ramat Aviv, 69978 Israel, [3]Laboratory for the Physics of Nanostructures, Ecole Polytechnique Fédérale de Lausanne, CH-1015 Lausanne, Switzerland and [4]Shemyakin-Ovchinnikov Institute of Bioorganic Chemistry, Russian Academy of Sciences, 117871 Moscow, Russia

Received August 31, 2005; Revised and Accepted October 31, 2005

ABSTRACT

The extension of the G-strand of long (700 bp) poly(dG)–poly(dC) by the Klenow exo$^-$ fragment of DNA polymerase I yields a complete triplex structure of the H-DNA type. High-performance liquid chromatography analysis demonstrates that the length of the G-strand is doubled during the polymerase synthesis. Fluorescence resonance energy transfer analysis shows that the 5′ ends of the G- and the C-strands, labeled with fluorescein and TAMRA, respectively, are positioned close to each other in the product of the synthesis. Atomic force microscopy morphology imaging shows that the synthesized structures lack single-stranded fragments and have approximately the same length as the parent 700 bp poly(dG)–poly(dC). CD spectrum of the polymer has a large negative peak at 278 nm, which is characteristic of the poly(dG)–poly(dG)–poly(dC) triplex. The polymer is resistant to DNase and interacts much more weakly with ethidium bromide as compared with the double-stranded DNA.

INTRODUCTION

Homopurine–homopyrimidine DNA sequences can adopt unusual triple-helical structures [reviewed in (1–3)]. Triplexes can be formed by a single DNA molecule (intramolecular triplexes) or by different molecules (intermolecular triplexes). Intramolecular triplexes (H-DNA) form when one of the strands of double-stranded DNA folds back to pair with the adjacent duplex [reviewed in (4)]. Formation of triplexes depends on chain length, base composition, divalent cations and temperature.

Poly(dG)–poly(dC) stretches incorporated into supercoiled plasmid DNA were shown to adopt various triplex structures (4–7). The poly(dG)–poly(dC) fragments introduced into the plasmid DNA have been shown to fold into halves from the center of the sequence to form a tetra-stranded-like structure. Spontaneous rearrangement of the two poly(dG) and the two poly(dC) parts of the tetra-stranded structure into triplex and a single-stranded motif took place under certain conditions. At neutral pH in the presence of Mg^{+2}, the G·G-C triplex was formed (6,7), whereas in the absence of Mg^{+2} in acidic conditions, when the C-strand becomes partially protonated, a C-G·C$^+$ triple helix was formed (4,5). In the G·G-C triplex, the two dG strands were running antiparallel to each other; in the C-G·C$^+$ triplex, the protonated dC$^+$ strand was running parallel to the dG one.

The presence of triplex structures was also detected in early preparations of poly(dG)–poly(dC), containing excess of (dG) nucleotide (8,9). CD spectroscopy analysis of poly(dG)–poly(dC) preparations obtained by *de novo* polymerase synthesis led Marck and Thiele (9) to the conclusion that the DNA samples comprised two hetero-complexes, double-stranded poly(dG)–poly(dC) and triple-stranded complex poly(dG)–poly(dG)–poly(dC). They have also shown that poly(dG)–poly(dC) samples of higher G-content were characterized by a higher relative concentration of triple-stranded structures. The calculated CD spectrum of poly(dG)–poly(dG)–poly(dC) triplex was different from that of the double-stranded poly(dG)–poly(dC) and was characterized by a large, negative peak at 278 nm (9).

We have recently demonstrated (10) that the extension of the $(dG)_{10}$–$(dC)_{10}$ oligonucleotide by the Klenow exo$^-$ fragment of DNA polymerase I in the presence of dGTP and dCTP

*To whom correspondence should be addressed. Tel: +972 3 640 7138; Fax: +972 3 640 6834; Email: s2shak@post.tau.ac.il

yields a long (up to 10 kb) double-stranded poly(dG)–poly(dC). Here, we report that the extension of the G-strand of the poly(dG)–poly(dC) by the Klenow exo$^-$ fragment of DNA polymerase I, under conditions when only the G-strand was allowed to grow, yields the complete poly(dG)–poly(dG)–poly(dC) triplex. Atomic force microscopy (AFM) morphology imaging analysis shows that these triplex structures have the same length but higher stiffness as compared with the parent poly(dG)–poly(dC).

MATERIALS AND METHODS

Materials

Unless otherwise stated, reagents were obtained from Sigma–Aldrich (USA) and were used without further purification. 2′-Deoxyribonucleoside 5′-triphosphates were purchased from Sigma–Aldrich. Klenow fragment exonuclease minus of DNA polymerase I from *Escherichia coli* lacking the 3′→5′exonuclease activity (Klenow exo$^-$) was purchased from Fermentas (Lithuania).

DNA samples

The oligonucleotides as well as fluorescein- (Flu) and tetramethylrhodamine- (TAMRA)-labeled oligonucleotides were purchased from Alpha DNA (Montreal, Canada). A total of 700 bp poly(dG)–poly(dC) and 220 bp labeled at both ends by the fluorescent dyes were synthesized from $(dG)_{10}$–$(dC)_{10}$ and 5′Flu-$(dG)_{12}$–5′TAMRA-$(dC)_{12}$, correspondingly, as described in our recent publication (10). Concentrations of dGTP and poly(dG)–poly(dC) (in base pairs) were calculated using extinction coefficients at 260 nm of 11.7 and 14.8 $mM^{-1}\,cm^{-1}$, correspondingly. CD spectra of poly(dG)–poly(dC) and triplexes were measured on the Aviv Model 202 series (Aviv Instrument Inc., USA) Circular Dichroism Spectrometer. Each spectrum was recorded from 220 to 320 nm and was an average of five measurements. Recording specifications were: wavelength step 0.5 nm, settling time 0.333 s, average time 1.0 s, bandwidth 1.0 nm and path length 1 cm.

DNA polymerase assays

A standard reaction mixture contained 60 mM K-Pi buffer, pH 7.4, 3 mM $MgCl_2$, 5 mM DTT, 1.5 mM dGTP, the Klenow exo$^-$ and 700 bp poly(dG)–poly(dC). The concentrations of poly(dG)–poly(dC) and Klenow exo$^-$ are noted in the legend to Figure 1. The reaction was started by the addition of the enzyme. The incubation was at 37°C for the times indicated in the figure legends. Reaction products were analyzed by size-exclusion high-performance liquid chromatography (HPLC) and by electrophoresis on an agarose gel.

HPLC separation of the polymerase products

The high molecular weight products of the synthesis were separated from nucleotides and other reaction components of the synthesis by using size-exclusion HPLC. The separation was carried out with a TSK-gel G-DNA-PW HPLC column (7.8 × 300 mm) from TosoHaas (Japan) by isocratic elution with 20 mM Tris-Acetate, pH 7.0, at a flow rate of 0.5 ml/min. Size-dependent separation of the strands that composed poly(dG)–poly(dC) and poly(dG)–poly(dG)–poly(dC) was performed using the same column by isocratic elution with 0.1 M KOH at a flow rate of 0.5 ml/min. The injection volumes were 40–150 µl. All experiments were conducted on an Agilent 1100 HPLC system, with a photodiode array detector. Peaks were identified from their retention times obtained from the absorbance at 260 nm. Data were collected from PDA and analyzed by Microsoft Excel.

Gel electrophoresis

The DNA samples were loaded onto 1% agarose gel and then electrophoresed at room temperature at 130 V for 1 h. TAE buffer, in addition to being used to prepare the agarose, also served as the running buffer. The dimensions of the agarose gel were 10 × 10 cm with 2 × 4 mm 14-wells. The gel was stained with ethidium bromide (0.5 µg/ml) and visualized with a Bio Imaging System 202D (302 nm). When indicated, the DNA samples were treated with 5 µg/ml DNase (Deoxyribonuclease I, EC 3.1.21.1) for 30 min at 37°C.

Fluorescence resonance energy transfer (FRET) measurements

Extension of fluorescently labeled oligonucleotides was performed in 100 mM Tris-Acetate, pH 8.0, 1.2 mM $MgCl_2$, 5 mM DTT, 1 mM dGTP, 20 µg/ml Klenow exo$^-$ and 0.2 µM Flu-$(dG)_{220}$–TAMRA-$(dC)_{220}$ duplex. The steady-state fluorescence measurements were carried out with Model LS50B Perkin-Elmer (England) Luminescence Spectrometer. Excitation was at 490 nm, with emission at 520 nm. The slits for excitation and emission monochromators were set at 5 and 10 nm, correspondingly.

Ethidium bromide fluorescence

Fluorescence measurements were performed in 20 mM Tris-Acetate, pH 7.0, containing 2 µM ethidium bromide and 10 µM (in base pairs or triads) DNA samples with Model LS50B Perkin-Elmer (England) Luminescence Spectrometer. Excitation was at 523 nm, with emission at 595 nm. The slits for excitation and emission monochromators were set at 5 and 15 nm, correspondingly.

Atomic force microscopy

AFM was performed on the molecules adsorbed onto mica surfaces. Aliquots containing 10–20 µl DNA samples in 2 mM Tris-Acetate, pH 7.0, containing 5 mM $MgCl_2$, were incubated on freshly cleaved moskovite mica plates for 10 min., washed with distilled water and dried with nitrogen gas. AFM images were obtained with a Veeco (USA) Nanoscope III multimode and PSIA (Korea) XE-100 AFMs in non-contact (tapping) mode, using high-resolution cantilevers (11) HRC (Nanotuning, Chernogolovka, Russia), or Si cantilevers (Micromash, Russia and Olympus, Japan). The images were 'flattened' (each line of the image was fitted to a second-order polynomial, and the polynomial was then subtracted from the image line) by AFM's image processing software to eliminate image distortions caused by sample tilt and scanner non-linearity. Length and height analysis were performed using a statistical image analysis program (DNACalc, NT-MDT, Russia).

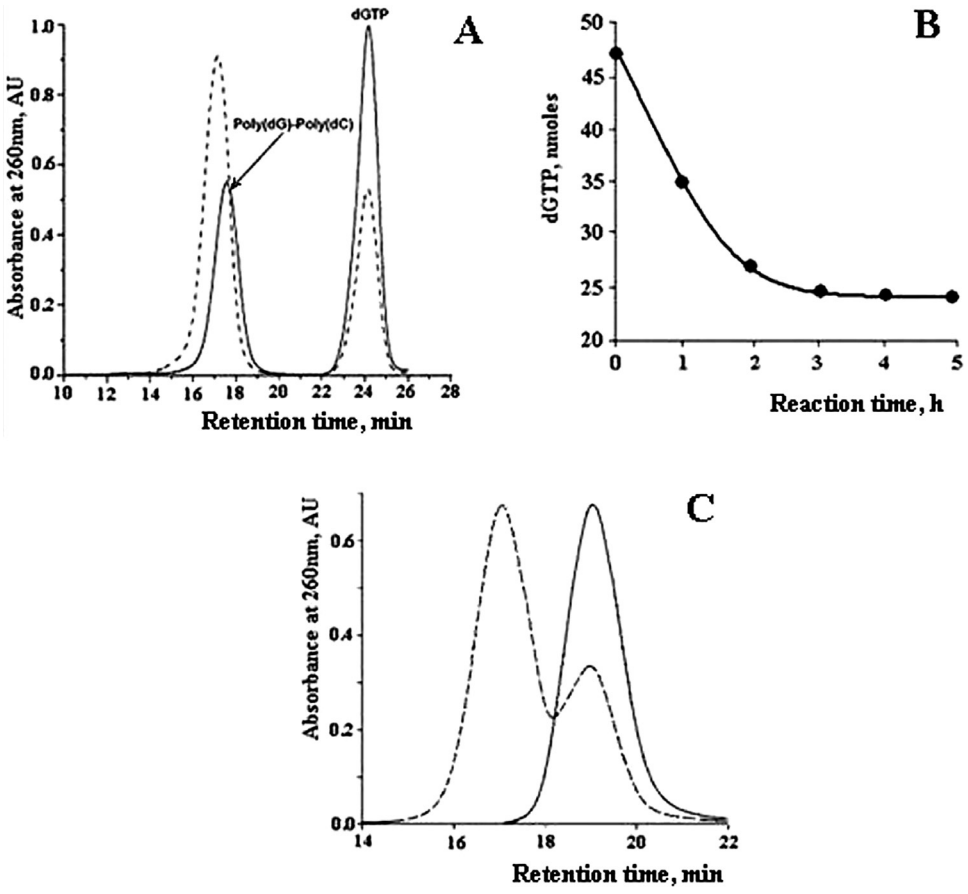

Figure 1. HPLC analysis of poly(dG–dG)–poly(dC) synthesis. (**A**) Size-dependent HPLC separation of the products of the synthesis. Polymerase extension assay was performed as described in 'Materials and Methods', with 2 μM 700 bp poly(dG)–poly(dC), 2.5 mM dGTP, 3.5 mM Mg^{2+} and 10 μg/ml Klenow exo$^-$ at 37°C. The reaction was started by addition of the enzyme. Aliquots of 50 μl were withdrawn from the assay mixture before (solid curve) and 3 h after (dashed curve) the addition of the enzyme, and loaded on TSKgel G-DNA-PW column (7.8 × 300 mm). Elution was performed with 20 mM Tris-Acetate buffer, pH 7.0, at a flow rate of 0.5 ml/min. (**B**) Time course of dGTP consumption. Polymerase extension assay was performed as described in (A). Aliquots were withdrawn from the assay after every hour and chromatographed as shown in (A). Nucleotide peaks from size-exclusion separations were collected and the amount of dGTP in the peaks was measured by absorption spectroscopy as described in 'Materials and Methods'. The amount of dGTP in the assay is plotted against time of synthesis. (**C**) Size-dependent HPLC of poly(dG)–poly(dC) and poly(dG–dG)–poly(dC) at high pH. Poly(dG–dG)–poly(dC) was synthesized as described in (A). Initial poly(dG)–poly(dC) (solid curve) and poly(dG–dG)–poly(dC) derived from extension of G-strand in the poly(dG)–Poly(dC) (dashed curve) were pretreated for 15 min at room temperature in 0.1 M KOH. A total of 100 (l of each DNA sample were applied onto TSKgel G-DNA-PW column (7.8 × 300 mm) and eluted with 0.1 M KOH at a flow rate of 0.5 ml/min.

RESULTS

Synthesis and characterization of poly(dG–dG)–poly(dC) triplex

Figure 1 depicts the synthesis of poly(dG)–poly(dG)–poly(dC) triplex from poly(dG)–poly(dC) by Klenow exo$^-$, conducted as described in 'Materials and Methods'. The products of the synthesis were analyzed by size-exclusion HPLC, as shown in Figure 1A. Incubation of 700 bp poly(dG)–poly(dC) with Klenow exo$^-$ and dGTP for 3 h results in growth of the poly(dG)–poly(dC) peak eluted before total column volume and slight shifting of its position to the left. The peak eluted from the column in total volume comprises dGTP; its height decreases together with the increase of the former peak. The above chromatographic behavior corresponds to incorporation of dG-nucleotides into the polymer. The peak eluted with total volume was collected and the quantity of dGTP was estimated by absorption spectroscopy. The dependence of the amount of dGTP in the assay on the time of the synthesis is shown in Figure 1B. As seen in Figure 1, dGTP content in the assay decreases with time; incorporation of dGTP into the polymer is halted when the amount of dGTP consumed becomes equal to the amount of G-bases in the starting poly(dG)–poly(dC). These data indicate that the initial length of G-strand of poly(dG)–poly(dC) increased twice during the synthesis. We performed direct length analysis of the strands composing the polymer by size-exclusion HPLC at high pH. At pH higher than 12.5, the poly(dG)- and the poly(dC)-strands are separated. As seen in Figure 1C (solid line), the G- and C-strands that compose poly(dG)–poly(dC) are eluted as a single peak from the column, thus proving that they are equal in size. Elution of products of the synthesis conducted for 3 h as described in Figure 1A is seen as two overlapped peaks (Figure 1C, dashed line). Analysis of the eluted fraction by absorption spectroscopy (not presented) shows that the earlier peak eluted between 16 and 18 min corresponds to the dG-homopolymer, while the peak eluted between 18 and 20 min corresponds to the dC-homopolymer. The C-strand is eluted

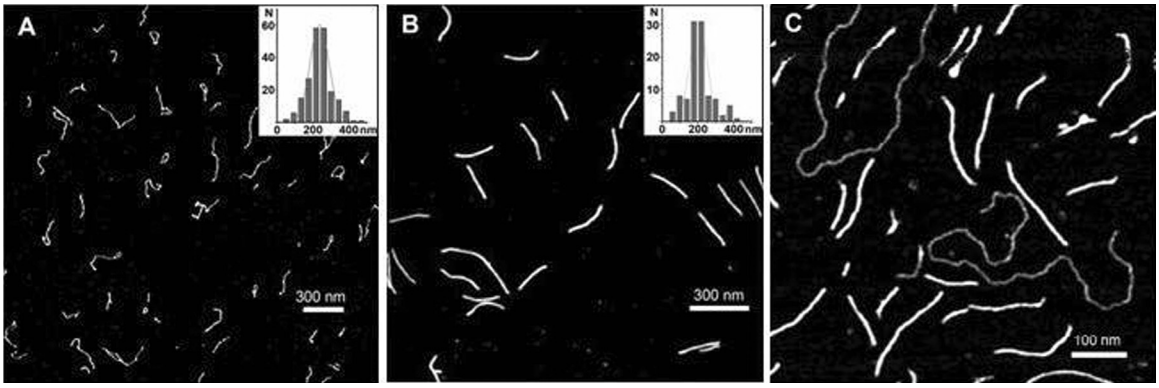

Figure 2. AFM images of (**A**) synthesized poly(dG–dG)–poly(dC) molecules (scale bar = 300 nm), (**B**) ~700 bp parent poly(dG)–poly(dC) (scale bar = 300 nm) and (**C**) poly(dG–dG)–poly(dC) molecules co-deposited with a linear plasmid pSK+ DNA (scale bar = 100 nm) on mica. The plasmid DNA on (C) can be easily distinguished due to its lower height (lower gray level) and much longer length. Statistical length analyses of single, well-separated molecules from several images at several areas are shown in the inserts to (A) and (B). The length values are corrected for the finite tip radius by subtracting the molecule's apparent width (a good approximation for the tip diameter) from the measured length, and yield an average value of 200 nm (SD = 20 nm) for poly(dG–dG)–poly(dC) (C) and 230 nm (SD = 45 nm) for poly(dG)–poly(dC).

from the column in a volume corresponding to that of 700 base strand, while the dG-strand is eluted in a volume corresponding to that of 1.5 kb strand (data not shown). Thus, the poly(dG)-strand composing the synthesized polymer is twice as long as the poly(dC)-strand; we will name this product poly(dG–dG)–poly(dC) throughout the study. It is generally accepted that intramolecular poly(dG)–poly(dG)–poly(dC) triplexes are stabilized by high (10–20 mM) concentrations of Mg-ions (4). Concentration of the cation in the assay (see 'Materials and Methods') was only 3 mM. We have also performed the synthesis in the presence of 10 mM Mg^{2+}, keeping concentrations of other components in the assay unchanged. The dG-strand extension in the presence of high Mg^{2+} was halted soon after the reaction had been started. The amount of dGTP incorporated into the dG-strand in the presence of 10 mM Mg^{2+} did not exceed 20% of the amount of dG-bases in the poly(dG)–poly(dC) (data not shown).

The 1 to 2 length ratio between the poly(dC)- and poly(dG)-strands in the product suggests that the dG-strand might fold back on itself, forming a compact paperclip-like triplex structure. Figure 2 presents data of AFM imaging and statistical analysis of the synthesized poly(dG–dG)–poly(dC) (panel A) and the parent poly(dG)–poly(dC) (panel B). The molecules were deposited on mica as described in 'Materials and Methods'. The average length of poly(dG–dG)–poly(dC) molecules, 200 ± 20 nm, is similar to that of poly(dG)–poly(dC) molecules, 230 ± 45 nm. Together with the absence of single-stranded fragments in the poly(dG–dG)–poly(dC), these data strongly indicate that the synthesized polymer is an intramolecular triplex. Morphological AFM analysis of the molecules presented in Figure 2C demonstrates height relations between poly(dG–dG)–poly(dC) and a standard double-stranded linear plasmid (pSK+) DNA co-deposited on the mica surface. The plasmid DNA is easily distinguished in the figure by its lower height (gray level) and much longer length. The estimated average apparent height, extracted from cross-sections of many molecules, of the triplex molecules, 1.2 ± 0.1 nm, is ~1.7 times higher than the average height of the plasmid DNA, 0.7 ± 0.1 nm. It reflects the larger diameter of the triplex molecules (12,13), as well as higher stiffness and resistance of poly(dG–dG)–poly(dC) structures to the surface adhesion forces and the pushing of the AFM tip (14). The height value of 0.6–0.7 nm is typical for double-stranded DNA measured on mica using AFM (14); these values are lower than the nominal diameter of the molecules in solution (larger than 2 nm) as a result of the molecules' interaction with the surface and the AFM tip.

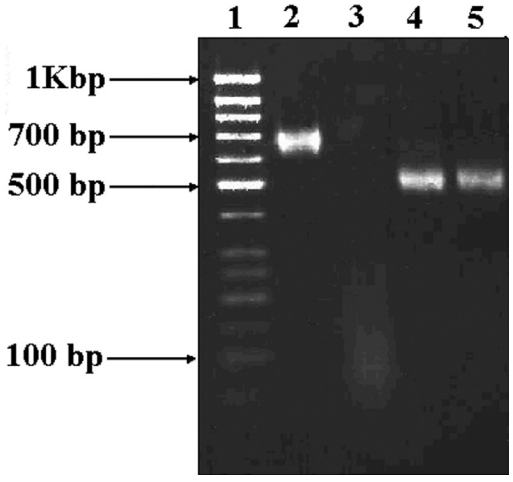

Figure 3. Mobility of poly(dG)–poly(dC) and poly(dG–dG)–poly(dC) molecules. Electrophoresis of the molecules in 1% agarose gel (see 'Materials and Methods'): molecular weights of 100 bp DNA-Ladder (lane 1) are indicated by left side arrows; poly(dG)–poly(dC) (lane 2); poly(dG)–poly(dC) treated for 30 min at 37°C with 5 μg/ml of DNase I (lane 3); poly(dG–dG)–poly(dC) (lane 4); poly(dG–dG)–poly(dC) treated for 30 min at 37°C with 5 μg/ml of DNase I (lane 5). Poly(dG–dG)–poly(dC) was synthesized as described in Figure 1. The electrophoresis was conducted for 1 h at 130 V. The amount of DNA loaded per lane was ~20 ng and the gel was ethidium bromide stained.

As seen in Figure 3, treatment of poly(dG–dG)–poly(dC) with DNase did not change the band position on the gel (compare lanes 4 with 5). Identical treatment of the starting poly(dG)–poly(dC) results in its complete cleavage by DNase, causing the disappearance of the corresponding band (compare lanes 2 with 3). Notice (compare lanes 2 with 4) that the

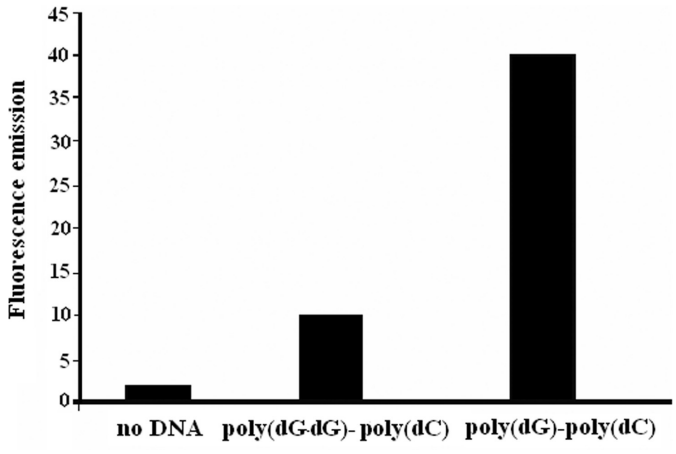

Figure 4. Interaction of poly(dG)–poly(dC) and poly(dG–dG)–poly(dC) with ethidium bromide. Fluorescence measurements were performed in 20 mM Tris-Acetate, pH 7.0 containing 2 μM ethidium bromide and 10 μM poly(dG)–poly(dC) (in base pairs) or 10 μM poly(dG–dG)–poly(dC) (in triads). Excitation was at 523 nm with emission at 595 nm. The slits for excitation and emission monochromators were set at 5 and 15 nm, correspondingly.

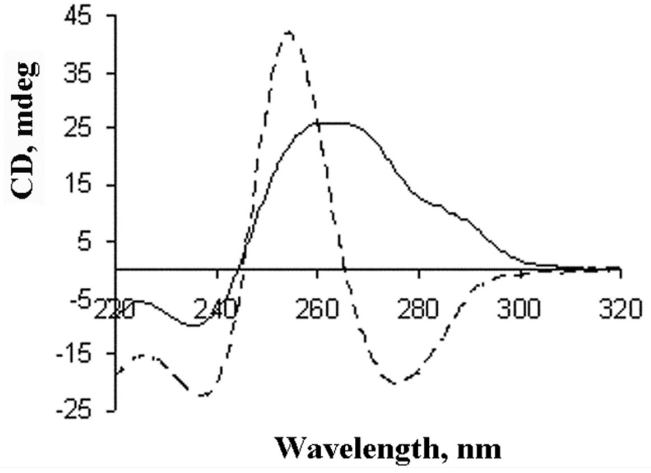

Figure 5. CD spectra of ~60 nM (concentration of molecules) poly(dG)–poly(dC) (solid curve) and poly(dG–dG)–poly(dC) (dashed curve) in 20 mM Tris-Acetate, pH 7.0 were recorded at 25°C. Each spectrum was recorded from 220 to 320 nm and was an average of five scans. Recording specifications were: wavelength step 0.5 nm, settling time 0.333 s, average time 1.0 s, bandwidth 1.0 nm and path length 1 cm.

poly(dG–dG)–poly(dC) band (lane 4) moves faster in the electric field and is less efficiently stained with ethidium bromide as compared with the poly(dG)–poly(dC) (lane 2). The reason for the faster movement is probably a higher charge density of the triplex as compared with that of the double-stranded DNA; different staining with ethidium is due to a different effect of the polymers on the dye fluorescence. Figure 4 presents data on interaction of ethidium bromide with poly(dG–dG)–poly(dC) and poly(dG)–poly(dC). As seen in the figure, interaction with poly(dG)–poly(dC) results in a 20-fold increase of the ethidium fluorescence emission. Only a 5-fold increase of the dye emission was observed when poly(dG–dG)–poly(dC) was used instead of poly(dG)–poly(dC). The resistance to DNase and the weaker effect on the ethidium fluorescence both suggest that the synthesized polymer adopts a conformation other than the double stranded. A data of CD spectroscopy presented in Figure 5 further proves that the synthesized poly(dG–dG)–poly(dC) is different from that of the double-stranded poly(dG)–poly(dC). CD spectra of poly(dG)–poly(dC) duplex and poly(dG–dG)–poly(dC) are considerably different. The spectrum of poly(dG–dG)–poly(dC) is characterized by a positive band at 250 nm and a negative band at 275 nm (see Figure 5, dashed curve). This spectrum is similar to the calculated spectrum for the triple-stranded poly(dG)–poly(dG)–poly(dC) motif (9).

The poly(dG–dG)–poly(dC), if exposed to high (more than 12) pH for 5–10 min and subsequently neutralized, undergoes an irreversible rearrangement. The alkali-treated polymer behaves differently on size-exclusion HPLC and is characterized by different optical and CD spectra, compared with a non-treated polymer (data not shown). Irreversible changes of poly(dG–dG)–poly(dC) at high pH are mainly due to the fact that both poly(dG)- and poly(dC)-strands, composing the polymer, have a tendency to form intra- and intermolecular homopolymeric structures, namely, double-stranded poly(dC):(dC+) (8,15,16) and poly(dG) quadruplexes (17,18).

FRET studies of poly(dG–dG)–poly(dC) synthesis

Direct evidence for the organization of the strands composing poly(dG–dG)–poly(dC) into intramolecular poly(dG)–poly(dG)–poly(dC) triplex of H-DNA type comes from the FRET analysis of the poly(dG)-strand extension, using poly(dG)–poly(dC) labeled at the 5′ ends of both strands with fluorescent dyes. FRET proved to be very useful for studies of various DNA and RNA structures, and for interaction of nucleic acids with proteins (19,20). In FRET, a donor fluorophore is excited by incident light and, if an acceptor is in close proximity, the excited state energy from the donor is transferred to it by means of intermolecular long-range dipole–dipole coupling (21). The efficiency of FRET is dependent on the inverse sixth power of the intermolecular separation between the donor and the acceptor. Thus, FRET provides a very sensitive measure of small changes in intermolecular distances. Flu energy donor and TAMRA energy acceptor moieties meet spectroscopic criteria that are important for the study of energy transfer (22). In these experiments, we used 220 bp poly(dG)–poly(dC) labeled at the 5′ end of the C-strand with TAMRA and at the 5′ end of the G-strand with Flu. Selection of a shorter (220 bp) polymer for FRET experiments was governed by the slower rate of G-strand extension in the labeled polymer. We have shown that extension of the G-strand in labeled 700 bp poly(dG)–poly(dC) by reasonable amounts (<50 μg/ml) of Klenow exo$^-$ takes tens of hours, which would make real-time FRET measurements of the dG-strand expansion using 700 bp poly(dG)–poly(dC) impractical. The distance between the 5′ ends in Flu-$(dG)_{220}$–$(dC)_{220}$-TAMRA is long enough (~60 nm) for the dyes not to communicate via FRET. Incubation of Flu-$(dG)_{220}$–$(dC)_{220}$-TAMRA with Klenow exo$^-$ and dGTP for 60 min resulted in a strong decrease of Flu emission at 520 nm, and in an increase of TAMRA fluorescence at 580 nm (see Figure 6B; notice that Figure 6A and B have different vertical scales). This is evident for efficient energy transfer between Flu and

TAMRA, and for a close proximity of the two chromophores in the synthesized product. Figure 7 presents the kinetics of Flu emission change during the synthesis. As seen in Figure 7 (left panel), incubation of Flu-$(dG)_{220}$–$(dC)_{220}$-TAMRA with GTP for 20 min did not result in decrease of the Flu emission. Further incubation of the polymer with Klenow exo$^-$ resulted in a stepwise reduction of the emission. The emission reached a certain level and then remained constant over a long time course. To explain the above behavior, the following scenario can be considered (see Figure 7, right panel): The first stage of the strand expansion resulted in the formation of a small overhang at the 5′ end of the poly(dG)-strand. The overhang is folded back on itself to form a poly(dG)–poly(dG)–poly(dC) motif at the distal DNA end. Further extension and folding back of the G-strand *de novo* results in the approach of the 5′ ends of the poly(dG)- and the poly(dC)-strands. This process cannot be followed up by FRET until the separation distance between the dyes attached to the 5′ ends reaches ~100 Å. The latter is due to the fact that no energy transfer takes place at distances >100 Å (19). Further reduction of the distance between the 5′ ends of the poly(dG)- and the poly(dC)-strands during the synthesis results in FRET between the dyes, and in a stepwise drop of the Flu emission. The expansion of the strand is halted at the time when the complete intramolecular triplex is formed. In the triplex, the dyes are positioned close to each other and therefore communicate efficiently by FRET.

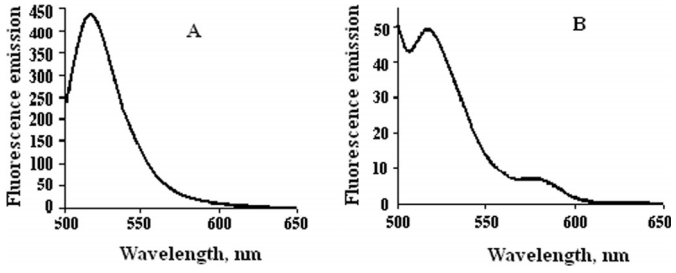

Figure 6. Fluorescence emission spectra of the product of Flu-$(dC)_{220}$–$(dG)_{220}$-TAMRA extension. Polymerase extension assay was performed in 100 mM Tris-Acetate, pH 8.0, 1.2 mM $MgCl_2$, 5 mM DTT, and 1.0 mM dGTP, 20 μg/ml Klenow exo$^-$ and 0.2 μM Flu-$(dG)_{220}$–TAMRA-$(dC)_{220}$ duplex at 37°C as described in 'Materials and Methods'. The spectra were recorded before (**A**), and 60 min after (**B**) initiation of the synthesis by addition of Klenow exo$^-$. Excitation was at 490 nm. Notice that (A) and (B) have different vertical scales.

DISCUSSION

Here, we report that the extension of the G-strand of 700 bp poly(dG)–poly(dC) by Klenow exo$^-$ fragment in the presence of dGTP yields a complete poly(dG–dG)–poly(dC) triplex. HPLC analysis of the synthesis products (see Figure 1) shows that the amount of dG-bases incorporated into the dG-strand during the synthesis is equal to the amount of dG-bases in poly(dG)–poly(dC); the length of the poly(dG)-strand is thus doubled during the synthesis. Direct AFM imaging of the molecular morphology (see Figure 2) shows that the poly(dG)–poly(dC) and the poly(dG–dG)–poly(dC) have almost the same length, and that no single-stranded fragments are present in the synthesized product. These data strongly indicate that the *de novo* G-strand is associated with the poly(dG)–poly(dC) duplex. FRET analysis shows (see Figure 7) that the 5′ ends of the poly(dG)- and the poly(dC)-strands in the synthesized polymer are positioned close to each other. This suggests that the poly(dG)-strand composing the polymer is folded back on itself and

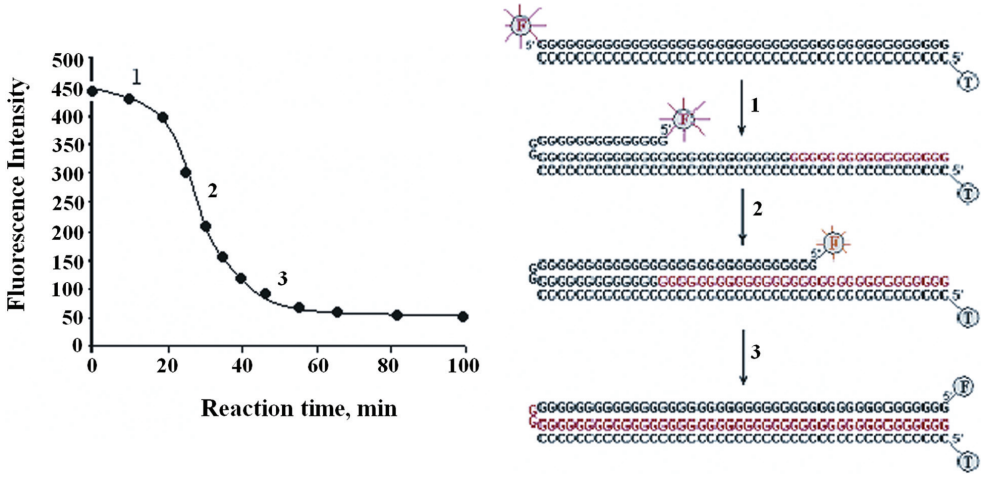

Figure 7. Left panel: kinetics of Flu emission change during the extension of G-strand of Flu-$(dC)_{220}$–$(dG)_{220}$-TAMRA by Klenow exo$^-$. The reaction was started by the addition of 20 μg/ml Klenow exo$^-$ to the cuvette containing 100 mM Tris-Acetate, pH 8.0, 1.2 mM $MgCl_2$, 5 mM DTT, 1.0 mM dGTP and 0.2 μM Flu-$(dG)_{220}$–TAMRA-$(dC)_{220}$ duplex and followed in time at 37°C by monitoring Flu emission at 520 nm; excitation was at 490 nm. Schematic presentation of the intermediate products of the synthesis is indicated to the right: F denotes for Flu, T for TAMRA. Emission of Flu in 220 bp long poly(dG)–poly(dC) is not quenched by TAMRA attached at the opposite end of the DNA molecule. Extension of the G-strand (new bases incorporated into the polymer are marked in red) results in folding the strand back and, as a result, in decrease of the molecular distance separating the dyes. This phase of the strand extension (phase 1) is not associated with a decrease of Flu emission, since the dyes are still positioned far away from one another and cannot communicate via FRET; further decrease of the separation distance (phase 2) results in FRET between the dyes and in a stepwise drop of the Flu emission. The expansion of the strand is stopped when a complete intramolecular triplex is formed (phase 3). In the triplex, the dyes are positioned close to one another and thus efficiently communicate via FRET.

is associated with the poly(dG)–poly(dC) The CD spectrum of the polymer is shown to be similar to that reported for the poly(dG)–poly(dG)–poly(dC) triplex motif (8). DNase does not cleave the polymer, and ethidium emission is much less affected by the polymer than by the double-stranded DNA. Putting all these data together, we can conclude that the synthesized product is an intramolecular poly(dG)–poly(dG)–poly(dC) triplex. Structures of this kind, known as H-DNA, have been originally reported for relatively short (tens of base pairs) poly(dG)–poly(dC) stretches that were introduced into supercoiled plasmid DNA (6). To the best of our knowledge, the hundreds of triads long nanostructures have never been previously reported. The average length of 700 triad triplexes reported here was approximately equal to 200 nm (see Figure 2). AFM morphology analysis shows that the triplex molecules are stiffer than the double-stranded DNA and manifest higher resistance to mechanical deformation by surface forces and the AFM tip compared with the double-stranded DNA (see Figure 2). We were able to produce longer triplex structures by extending the dG-strand of longer parent poly(dG)–poly(dC), using the same procedure as described in 'Materials and Methods' (data not shown).

Rao and co-workers (23) have studied extension of synthetic $(dG)_{30}$–$(dC)_{30}$ nucleotides by the Klenow exo$^-$ fragment of polymerase I. Extension of dG-strand by polymerase in the presence of dGTP in their case did not yield a complete $(dG)_{30}$–$(dG)_{30}$–$(dC)_{30}$ triplex; the dG-strand expansion was halted after the addition of only 5–10 bases to the dG-strand of $(dG)_{30}$–$(dC)_{30}$. The results presented herein, however, demonstrate the synthesis of long, complete poly(dG)–poly(dG)–poly(dC) by Klenow exo$^-$. The synthesis in our case was halted when the length of the dG-strand was doubled. In order to understand the reason for this discrepancy, we performed the synthesis under conditions similar to those carried out by Rao and co-workers (23), who used 10 mM Mg^{+2} in the assay, while we used only 3.5 mM. Indeed, when we conducted extension of the dG-strand of 700 bp poly(dG)–poly(dC) in the presence of 10 mM Mg^{+2}, the dG-strand synthesis was halted long before doubling of the strand; the G-strand length was extended by no more than 20%. We also observed that this synthesis, if conducted in the presence of 10 mM Mg^{+2}, resulted in the formation of high molecular weight DNA structures in the assay. These structures behaved as 2–3 kb DNA in both size-exclusion HPLC and electrophoresis (data not shown). We suggest that, in the presence of high concentrations of Mg^{+2}, the dG-strand fragments synthesized *de novo* interact with each other to form stable, intermolecular four-stranded dG-quadruplex structures, thus connecting four poly(dG)–poly(dC) molecules together. This suggestion is supported by the fact that 10–20 mM Mg^{+2} induces self-assembly of dG-rich sequences (24) and formation of dG-rich structures in plasmids containing $(dG)_n$–$(dC)_n$ inserts (25). Formation of these quadruplex structures might be also the reason for the early termination of G-strand extension by polymerase.

ACKNOWLEDGEMENTS

This work is supported by a European Grant for Future & Emerging Technologies (IST-2001-38951). Funding to pay the Open Access publication charges for this article was provided by a European Grant for Future and Emerging Technologies (IST-2001-38951).

Conflict of interest statement. None declared.

REFERENCES

1. Frank-Kamenetskii,M.D. and Mirkin,S.M. (1995) Triplex DNA structures. *Annu. Rev. Biochem.*, **64**, 65–95.
2. Sun,J.S., Garestier,T. and Helene,C. (1996) Oligonucleotide directed triple helix formation. *Curr. Opin. Struct. Biol.*, **6**, 327–333.
3. Radhakrishnan,I. and Patel,D.J. (1994) DNA triplexes: solution structures, hydration sites, energetics, interactions, and function. *Biochemistry*, **33**, 11405–11416.
4. Frank-Kamenetskii,M.D. and Mirkin,S.M. (1994) H-DNA and related structures. *Annu. Rev. Biochem.*, **23**, 541–576.
5. Lyamichev,V.I., Mirkin,S.M. and Frank-Kamenetskii,M.D. (1987) Structure of $(dG)_n.(dC)_n$ under superhelical stress and acid pH. *J. Biomol. Struct. Dynam.*, **5**, 275–282.
6. Kohwi,Y. and Kohwi-Shigematsu,T. (1988) Magnesium ion-dependent triple-helix structure formed by homopurine–homopyrimidine sequences in supercoiled plasmid DNA. *Proc. Natl Acad. Sci. USA*, **85**, 3781–3785.
7. Kohwi-Shigematsu,T. and Kohwi,Y. (1991) Detection of triple-helix related structures adopted by poly(dG)–poly(dC) sequences in supercoiled plasmid DNA. *Nucleic Acids Res.*, **19**, 4267–4271.
8. Marck,C., Thiele,D., Schneider,C. and Guschlbauer,W. (1978) Protonated polynucleotides structures—22.CD study of the acid–base titration of poly(dG).poly(dC). *Nucleic Acids Res.*, **5**, 1979–1996.
9. Marck,C. and Thiele,D. (1978) Poly(dG).poly(dC) at neutral and alkaline pH: the formation of triple stranded poly(dG).poly(dG).poly(dC). *Nucleic Acids Res*, **5**, 1017–1028.
10. Kotlyar,A.B., Borovok,N., Molotsky,T., Fadeev,L. and Gozin,M. (2005) *In vitro* synthesis of uniform poly(dG)–poly(dC) by Klenow exo$^-$ fragment of polymerase I. *Nucleic Acids Res.*, **33**, 525–535.
11. Klinov,D. and Magonov,S. (2004) True molecular resolution in tapping-mode atomic force microscopy with high-resolution probes. *Applied physics letters*, **84**, 2697–2699.
12. Rhee,S., Han,Z., Liu,K., Miles,H.T. and Davies,D.R. (1999) Structure of a triple helical DNA with a triplex-duplex junction. *Biochemistry*, **38**, 16810–16815.
13. Vlieghe,D., Meervelt,L.V., Dautant,A., Gallois,B., Précigoux,G. and Kennard,O. (1996) Parallel and antiparallel $(G{\cdot}GC)_2$ triple helix fragments in a crystal structure. *Science*, **273**, 1702–1705.
14. Kasumov,A., Klinov,D., Roche,P.-E., Gueron,S. and Bouchiat,H. (2004) Thickness and low-temperature conductivity of DNA molecules. *Appl. phys. Lett.*, **84**, 1007–1009.
15. Gray,D.M. and Bollum,F.J. (1974) A circular dichroism study of poly dG, poly dC, and poly dG:dC. *Biopolymers*, **13**, 2087–2102.
16. Thiele,D., Marck,C., Schneider,C. and Guschlbauer,W. (1978) Protonated polynucleotides structures–23. The acid–base hysteresis of poly(dG).poly(dC). *Nucleic Acids Res.*, **5**, 1997–2012.
17. Davis,J.T. (2004) G-quartets 40 years later: from 5′-GMP to molecular biology and supramolecular chemistry. *Angew. Chem. Int.*, **43**, 668–698.
18. Simonsson,T. (2001) G-quadruplex DNA structures—variations on a theme. *Biol. Chem.*, **382**, 621–628.
19. Clegg,R.M. (1992) Fluorescence resonance energy transfer and nucleic acids. *Methods Enzymol.*, **211**, 353–388.
20. Lilley,D.M. and Wilson,T.J. (2000) Fluorescence resonance energy transfer as a structural tool for nucleic acids. *Curr. Opin. Chem. Biol.*, **4**, 507–517.
21. Stryer,L. (1978) Fluorescence energy transfer as a spectroscopic ruler. *Annu. Rev. Biochem.*, **47**, 819–846.
22. Wu,P. and Brand,L. (1994) Resonance energy transfer: methods and applications. *Anal. Biochem.*, **218**, 1–13.
23. Karthikeyan,G., Chary,K.V.R. and Rao,B.J. (1999) Fold-back structures at the distal end influence DNA slippage at the proximal end during mononucleotide repeat expansions. *Nucleic Acids Res.*, **27**, 3851–3858.
24. Chen,F.M. (1997) Supramolecular self-assembly of $d(TGG)_4$, synergistic effects of K+ and Mg^{2+}. *Biophys. J.*, **73**, 348–356.
25. Panyutin,I.G., Kovalsky,O.I. and Budowsky,E.I. (1989) Magnesium-dependent supercoiling-induced transition in $(dG)_n.(dC)_n$ stretches and formation of a new G-structure by (dG)n strand. *Nucleic Acids Res*, **20**, 211–215.